International Journal of Nanoelectronics and Materials
Volume 15 (Special Issue) December 2022 [367-374]

Simulation of InGaAs-Based Self-Switching Diodes as Sub-Terahertz Rectifiers

F. Aziz[1,*], S.R. Kasjoo[1], N.F. Zakaria[1,2], Fauzi Packeer[3] and A.K. Singh[4]

[1]Faculty of Electronic & Technology Engineering, Universiti Malaysia Perlis (UniMAP), Arau 02600, Perlis, Malaysia
[2]Advanced Communication Engineering, Centre of Excellence (ACE), Universiti Malaysia Perlis (UniMAP), Kangar 01000, Perlis, Malaysia
[3]School of Electrical and Electronic Engineering, Universiti Sains Malaysia, Nibong Tebal 14300, Malaysia
[4]Department of Electronics and Communication Engineering, Punjab Engineering College (Deemed to be University), Sector-12, Chandigarh 160012, India

ABSTRACT

Abstract. A self-switching device (SSD) is a new device concept -which can be simply realized by forming insulating trenches into a semiconductor layer, using a single nanolithography process. SSDs can be utilized as rectifiers since the device's current-voltage (I-V) characteristic is comparable to that of a conventional diode. The simulation of two InGaAs-based SSDs with parallel connection using ATLAS device simulator for similar and different lengths of both SSDs (L_1 and L_2) is presented in this paper. The simulation results show that the InGaAs-based SSDs are able to operate up to sub-terahertz (THz) frequencies. As expected, lowering either L_1 or L_2 will not only increase the device's cut-off frequency, f_c, but also degrading the device's rectification performance (i.e., reducing the value of curvature coefficient, γ). The highest cut-off frequency achieved in this work was 0.27 THz with γ ~18 V^{-1} when L_1 = 0.8 μm and L_2 = 0.4 μm.

Keywords: Diode, self-switching diode, terahertz frequency, curvature coefficient

1. INTRODUCTION

Due to a very wide spectrum of possible applications for next-generation computation and communication, terahertz (THz) technology has received a fast-growing attention [1]. In recent decades, developing high-speed detectors with highly sensitive, low-cost, high-throughput, easily portable and the potential to integrate numerous devices has become a major research area. However, this field of study is still in its early stages [2]. The development of solid-state, compact, room-temperature emitters and detectors is one of the major challenges in the THz frequency range [3]. Conventional p-n junction diodes cannot be used as a rectifier for THz frequency applications due to the lag caused by the majority carriers' delayed transition. Therefore, the focus of high frequency area utilisation has been on devices with a unipolar or majority carrier, such as tunnel diodes, back diodes, and Schottky diodes [4]. Tunnel diodes and back diodes have not been used as frequently as mixers and detectors at microwave frequencies because of a higher susceptibility to radio frequency (RF) burnout, circuit complexity, and manufacturing challenges [5]. An alternative approach to use a device for high frequency is the self-switching device (SSD), which is a unipolar rectifying diode at the nanoscale size. By forming insulating trenches into a semiconductor layer, an SSD can be produced in a single nanolithography process. Figure 1(a) depicts the atomic force microscope (AFM) image of a single SSD with an anode and cathode-connected narrow channel constructed between two (etched) L-shaped insulating trenches. At zero bias where the supply voltage, V = 0, the depletion regions are induced at the insulator-semiconductor interface as illustrated in Figure 1(b). By applying V > 0 will reduce the depletion

* faradilla@unimap.edu.my

regions due to electrostatic effects as in Figure 1(c) resulting in allowing current to pass through the channel of the device. The depletion regions will enlarge, as shown in Figure 1(d), when V < 0 is applied, and the channel will eventually closed, preventing current from flowing across the device. The current-voltage (I-V) characteristic of a single SSD, as shown in Figure 1(e), illustrates how this results in the realisation of the functionality of a diode. This SSD is a completely novel device design because it does not rely on a standard diode's doping (p-n) junction or energy barrier structure [6].

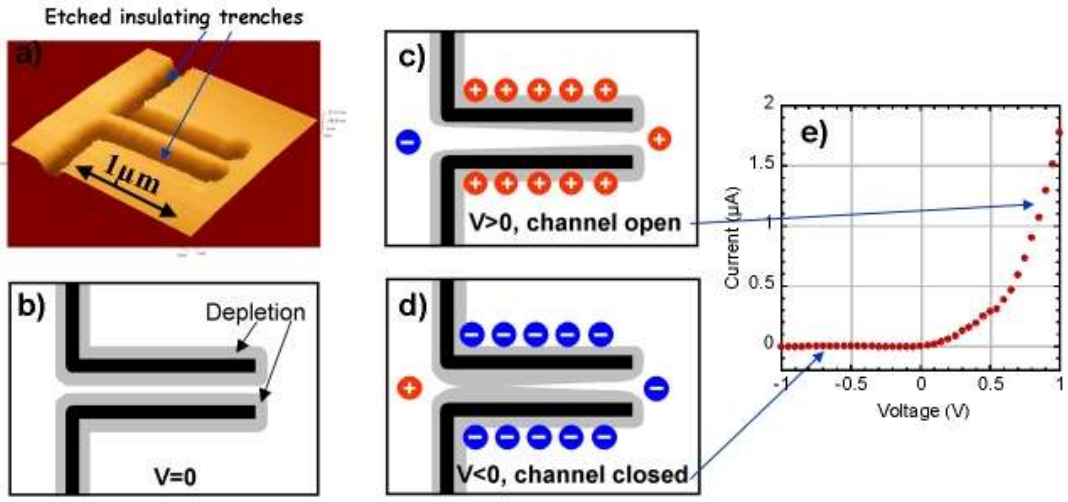

Figure 1. (a) An AFM image of a single SSD. (b) The grey area (native depletion region) was formed using etched interfaces. (c) Applying positive voltage will open the device channel. (d) Applying negative voltage will close the device channel. (e) Single SSD I-V characteristics [6].

1.1 Two Parallel InGaAs Self-Switching Diode Simulations

Figure 2 illustrate the top-view structure of two InGaAs-based SSDs with parallel connections. Anode and cathode connections were made for these parallel SSDs on the left and right, respectively. Both L-shaped SSDs were constructed using In0.7Ga0.3As as the substrate and air as the insulator. This structure with parameters such as the device lengths, L_1 and L_2, for top and bottom SSDs, respectively, the device channel width, W, and the device trench width, W_t, has been used in this work. For this simulation, electrical parameters with values of 1 x 10^{17} cm^{-3} for uniform n-type doping, -3.75 x 10^{11} cm^{-2} for interface charge density, 1 x 10^{-8} Ω cm^2 for contact resistivity, and 12,000 cm^{-2} V^{-1} s^{-1} for electron mobility without scattering, and 300 K for temperature were utilized.

Previous results reported by Zakaria et. al. on a single InGaAs-based SSD using ATLAS device simulator have been used to validate our simulation in which the dimension parameters of the device were set as the followings; the device channel length and width are 0.8 μm and 0.07 μm, respectively, and W_t = 0.05 μm [7]. The obtained I-V characteristic of the device and the curvature coefficient, γ, versus voltage graph were comparable. Both results can be viewed in Figure 3(a) and 3(b), respectively.

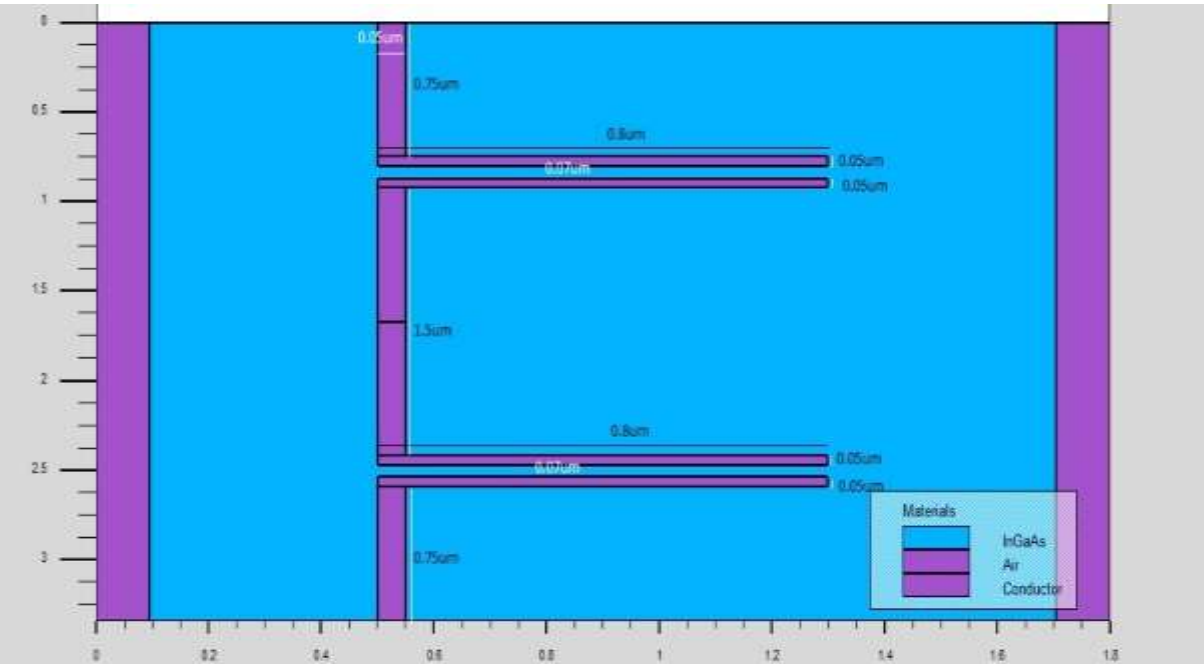

Figure 2. Two InGaAs-based SSDs connected in parallel dimensions.

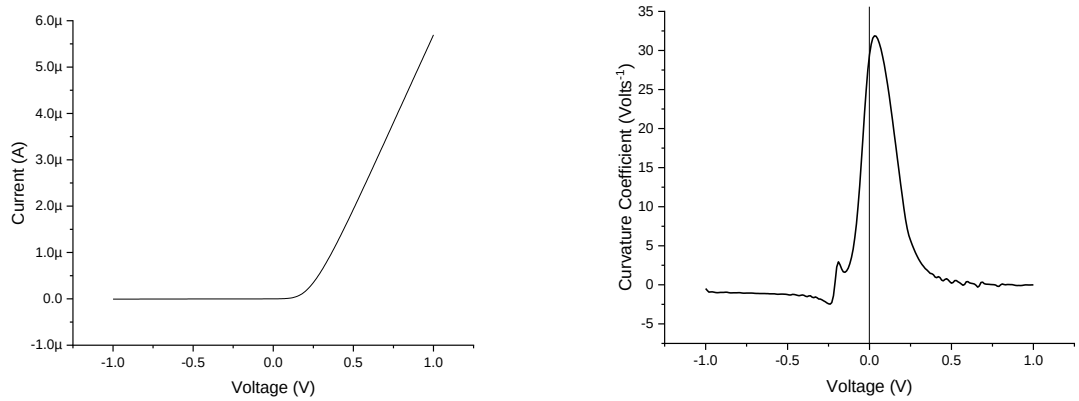

Figure 3. (a) Validation I-V behavior. (b) Validation of curvature coefficient.

The simulations were then conducted for different channel length combinations whereby L_1 was fixed at 0.8 µm and L_2 was varied at 0.8 µm, 0.6 µm and 0.4 µm. Other parameters such as W and W_t were fixed at 0.07 µm and 0.05 µm, respectively.

1.2 Device Characteristic

A bias voltage of 0 V and an input signal from an AC source with an amplitude of 0.5 V were applied to the device at various frequencies. To determine the cutoff frequency (f_c) of the device, the calculation of mean output current of an AC transient analysis was performed and plotted for each simulated frequency. Equation (1) is then used to get the mean of the output current.

$$I_{mean} = \frac{1}{t_1 - t_i}\int_{t_i}^{t_1} f(t_1)dt - \frac{1}{t_2 - t_1}\int_{t_1}^{t_2} f(t_2)dt \quad (1)$$

with,

$$t_2 = t_1 - T \tag{2}$$

where t_i is the initial time, t_1 is the transition between the positive and negative cycle, T is the period, and dt is the discrete transition time of the simulation. The point at which the sinusoidal positive output waveform equals the sinusoidal negative output waveform ($I_{mean} = 0$) is where f_c is estimated. The f_c can be compared with the theoretical calculation by using the equation below:

$$f_c = \frac{1}{2\pi R_s C} \tag{3}$$

where C is the SSD's capacitance and R_s is its serial resistance. Details regarding R_s and C value can be found in [8] and [9]. The rectified voltage, Δυ can be written as in a simple small signal analysis and can be expressed as

$$\Delta\upsilon = \frac{A^2 f^{(2)}}{4f^{(1)}} \tag{4}$$

where A represents the input signal's amplitude and f(1) and f(2) represent the device's I-V behavior's first and second order derivatives, respectively. Since A is fixed, the rectified voltage is proportional to the $f^{(2)}$ and $f^{(1)}$ ratio.

$$\Delta\upsilon \propto \frac{f^{(2)}}{f^{(1)}} \tag{5}$$

The curvature coefficient, γ, is the ratio that determines how well the device performs rectification [4, 10, 11].

2. RESULTS AND DISCUSSION

I-V characteristics of several pair channel lengths are shown in Figure 4(a), including L_1 = 0.8 μm/ L_2 = 0.8 μm (labelled as L0.8_L0.8), L_1 = 0.8 μm/ L_2 = 0.6 μm (labelled as L0.8_L0.6) and L_1 = 0.8 μm/ L_2 = 0.4 μm (labelled as L0.8_L0.4), together with their corresponding γ in Figure 4(b). The amount of current flowing across the device will double when two SSDs are connected in parallel, as seen in Figure 4(a). Shorter channels will give shorter transmission channels for carriers to transmit across the device, hence it is expected that a parallel SSDs with L0.8_L0.4 results in the higher amount of current at any applied voltage when compared to other combinations with higher length (i.e., L0.8_L0.6 and L0.8_L0.8). Moreover, parallel SSDs with L0.8_L0.4 also displayed a smaller turn-on voltage, V_t, closer to zero volt than other channel length combinations. However, the highest current leakage at V = -1 V with the value of 1.34 μA can be observed for parallel SSDs with L0.8_L0.4, due to the short channel effect. It is expected that decreasing the V_t with will increase the short-channel effect. Leakage current, which is produced by the reverse-bias voltage and is a tiny amount of current that passes through the diode, is usually negligible. Parallel SSDs with L0.8_L0.6 and L0.8_L0.8 showed the leakage current has decreased as can be seen in Figure 4(a). It is worth to notice that the value of V_t and γ increase as the value of L_2 increases as shown in Figure 5. These results are comparable to observation reported by Zakaria et. al on the rectification performance of InGaAs-based SSDs, which found that the performance has a substantial relationship with V_t and reverse current [12].

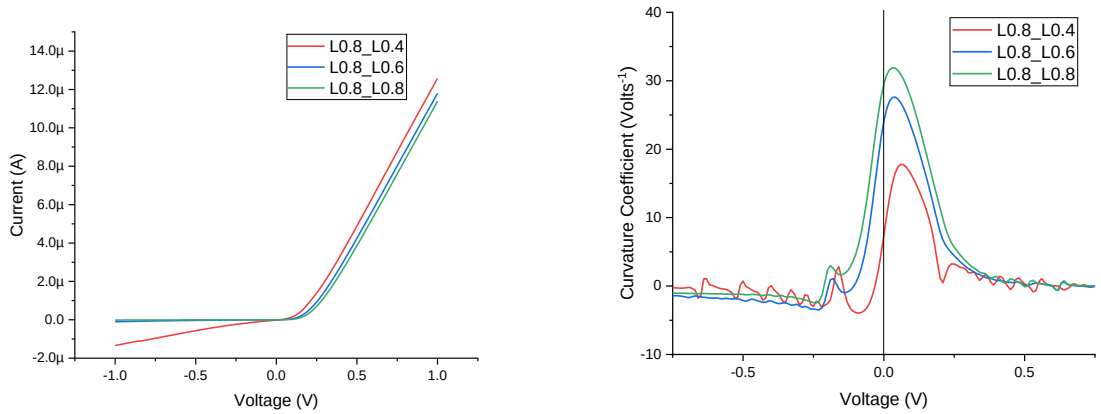

Figure 4. (a) I-V behavior of parallel InGaAs SSDs and (b) Rectification performance measured by the device curvature coefficient in relation to the applied voltage for different pair channel lengths.

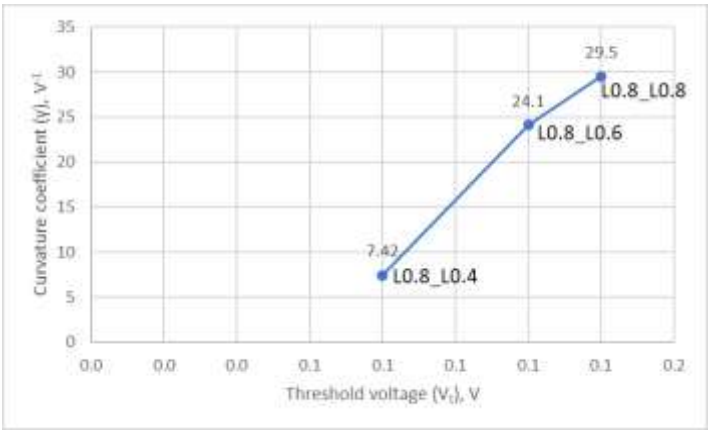

Figure 5. Graph γ versus V_t.

The performance of the parallel SSDs was then evaluated using AC transient analysis for a range of frequencies including 1 GHz, 10 GHz, and 100 GHz using a 0.5 V sinusoidal input. Rectification appears to be effective at 1 GHz frequency because the output current is in phase with the applied input voltage as shown in Figure 6(a), as predicted by based on the I-V behavior, the parallel SSDs with L0.8_L0.4 displayed the largest output current due to its V_t being the closest to 0 V. Higher frequencies of 10 GHz and 100 GHz, as seen in Figures 6(b) and 6(c), respectively, caused the output current to begin to de-phase (with respect to the input signal).

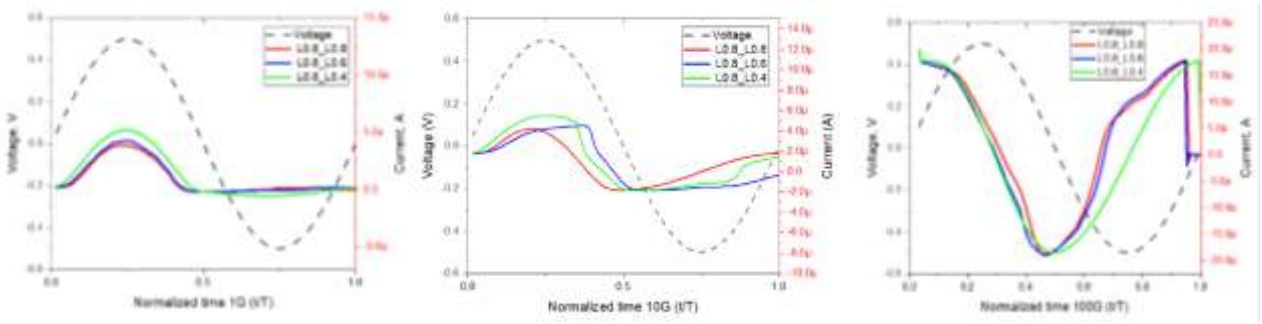

(a) (b) (c)

Figure 6. AC transient analysis of parallel SSDs at frequencies of (a) 1 GHz, (b) 10 GHz, and (c) 100 GHz for different pair channel lengths.

By plotting the I_{mean} calculated using equation (1) against input voltage frequency of several simulated frequencies, the f_c for each parallel SSDs can be estimated as shown in in Figure 7. According to the data, parallel SSDs with L0.8_L0.4 have the highest cut-off frequency, which is around 0.27 THz. Increasing L_2 to 0.6 µm and 0.8 µm will reduce the value of f_c 0.23 THz and 0.17 THz respectively.

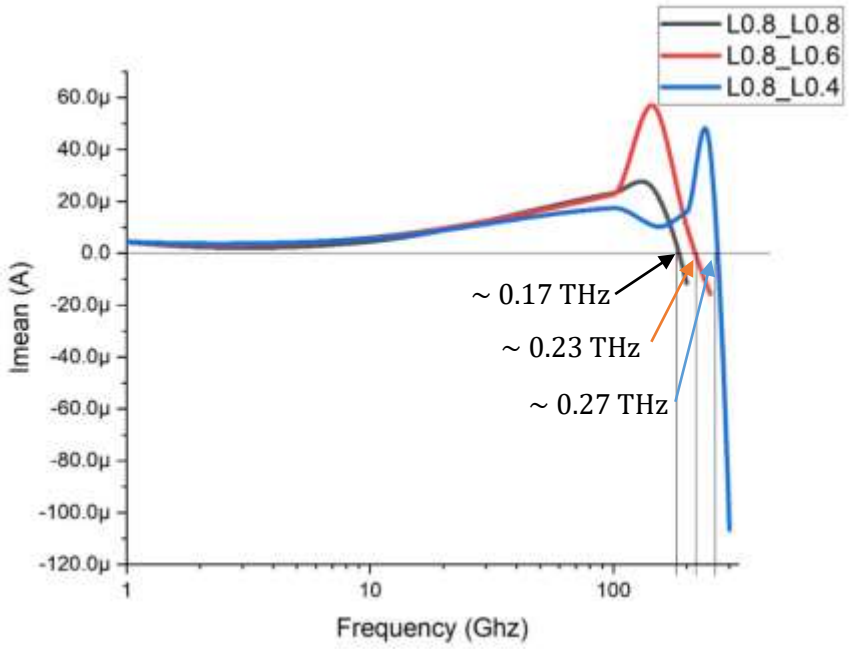

Figure 7. Mean output current, I_{mean}, and the cut-off frequency, f_c, results for various pair channel lengths.

Table 1 shows the calculated and estimated f_c of the SSDs with various pair channel lengths. The results indicate that the simulated and theoretical f_c are nearly identical. The theoretical approach to estimate the value of f_c is based on the standard equation of cut-off frequency with R_s and C value can be calculated by referring to [8] and [9].

Table 1 Tabulated data of estimated cut-off frequency, f_c based on simulation and theoretical calculation

Parallel SSDs length,L (μm)	Simulated cut-off frequency (THz)	Theoretical cut-off frequency (THz)	Percentage difference (%)	Leakage Current at reverse bias (μA)	Rectification Performance, γ ($Volts^{-1}$)
0.8/0.4 μm	~0.27	0.263	2.6	1.34	~18
0.8/0.6 μm	~0.23	0.228	0.9	0.10	~27
0.8/0.8 μm	~0.17	0.263	17.5	0.01	~32

3. CONCLUSION

The simulations of two parallel InGaAs-based SSDs using ATLAS design device simulator for identical and different lengths of both SSDs operating up to sub-THz frequencies were presented. In this work, the maximum cut-off frequency achieved for parallel SSDs is approximately ~0.27 THz with curvature coefficient of ~18 V^{-1} for L_1 = 0.8 μm and L_2 = 0.4 μm. The effects of changing the value of L_2 have also been discussed, which can be used as a reference in realizing enhancing the performance of SSD-based rectifiers.

ACKNOWLEDGEMENTS

The authors would like to acknowledge support from the Fundamental Research Grant Scheme (FRGS) under grant number FRGS/1/2019/STG02/UNIMAP/03/1 from the Ministry of Higher Education Malaysia.

REFERENCES

[1] C. Balocco et al., Novel Terahertz nanodevices and circuits, 2010 10th IEEE International Conference on Solid-State and Integrated Circuit Technology, 2010, pp. 1176-1179.
[2] Takahito Ohshiro, Nanodevices for Biological and Medical Applications: Development of Single-Molecule Electrical Measurement Method, in Appl. Sci., vol 12 issue 3 (2022).
[3] Pickwell, E., and V.P. Wallace. Biomedical applications of terahertz technology. Journal of Physics D: Applied Physics 39.17 (2006): R301.
[4] Self-switching diodes as RF rectifiers: evaluation methods and current progress. Bulletin of Electrical Engineering and Informatics, (2019).
[5] M.A. Laughton and D.F. Warne. Power semiconductor devices. Electrical engineer's reference book (2003) pp. 25-27.
[6] Song, A.M., Missous, M., Omling, P., Peaker, A.R., Samuelson, L., Seifert, W., Appl. Phys. Lett. vol 83, issue 9 (2003) pp. 1881-1883.
[7] N.F. Zakaria, S.R. Kasjoo, M.M. Isa, Z. Zailan, M.B.M. Mokhtar, and N. Juhari, AIP Conf. Proc. vol. 2203, issue 1 (2020).
[8] Aberg, M, and Saijets, J., DC and AC Characteristics and modelling of Si SSD-nano devices in Proc. Of the European Conference on Circuit Theory and Design, vol 1, (2005).
[9] Lien, C.D., F.C.T., and Nicolet, M. -A, An Improved Forward I-V Method for Nonideal Schottky Diodes with High Resistance, in IEEE Transaction on Electron Device, vol 31, issue 10 (1984), pp. 1502-1503.
[10] S.R. Kasjoo, A.K. Singh, and A.M. Song, RF Characterization of unipolar nanorectifiers at zero bias, in Physica Status Solidi (a), vol 212 issue 9 (2015), pp. 2091-2097.
[11]

[12] N.F. Zakaria, Z. Zailan, M.M. Isa, S. Taking, M.K.M. Arshad and S.R. Kasjoo, Permittivity and temperature effects to rectification performance of self-switching device using two-dimensional simulation, 2016 5th International Symposium on Next-Generation Electronics (ISNE), 2016, pp. 1-2.

[13] N.F. Zakaria, S.R. Kasjoo, Z. Zailan, M.M. Isa, S. Taking, M.M.M Arshad., Permittivity and temperature effects on rectification performance of self-switching diodes with different geometrical structures using two-dimensional simulation device simulator, in Solid-State Electronics, vol 138 (2017), pp. 16-23.